



# Effect of Nepheline Syenite Additives on the Technological Behavior of Ceramics and Porcelain Stoneware Tiles

M. S. Elmaghraby<sup>1</sup> · A. I. M. Ismail<sup>2</sup> · D. Sadek Ghabrial<sup>2</sup> · Z. A. Abd El-Shakour<sup>2</sup>

Received: 7 April 2019 / Accepted: 13 June 2019 / Published online: 21 June 2019  
© Springer Nature B.V. 2019

## Abstract

To study the effect of the Egyptian nepheline syenite raw materials on the sinterability of the ceramic tiles, four batches with concentrations of nepheline syenite (0, 5, 10 and 15%) were prepared. The four batches were ground, mixed, shaped, pressed and fired at temperatures from 1160 °C to 1260 °C. Some technological behaviors of the samples were measured in dry, green state and after firing at 1260 °C; including densification parameters. Phase composition and microstructural studies referred that mullite was the newly crystallized phase after firing set in a glassy matrix enriched in alkalis. Technological properties of the fired batches revealed that the higher firing temperature and higher nepheline syenite contents produced larger amounts of glassy phase, and consequently bulk density and linear shrinkage increased, while apparent porosity and water adsorption as well as whiteness of fired batches decreased. It is concluded that nepheline syenite could be successfully used as flux in ceramic tiles, while it is not accepted in the production of porcelain bodies because of their coloration.

**Keywords** Ceramic tiles · Porcelain bodies · Nepheline syenite

## 1 Introduction

Porcelain stoneware bodies composed essentially of mixtures from ball clay, kaolin, quartz and feldspars, which have different amounts of Na<sub>2</sub>O and K<sub>2</sub>O, fired at temperatures ranging from 1200 °C to 1300 °C. However, the optimization of sanitaryware porcelain production requires further improvement with regard to ceramic structures and properties. For the role of the clay and kaolin, dissociation reactions of the clay minerals, water loss and formation of the new phases (e.g. meta-kaolin, mullite and glassy silica) are achieved during firing. Further, quartz acts as a filler to support the tiles and forms the siliceous viscous liquid at higher temperature [1–2].

Feldspars in their two forms represented by sodic and potassic types are namely albite and orthoclase and /or microcline, respectively. These feldspars play the essential role as the fluxing materials in the ceramic tile industries and exist in pegmatites as native veins or as components within other rocks as granite and syenite in addition to the placers deposits. Sodic feldspar has a lower melting point than potassic one so the added ratio of each type should be carefully calculated to adjust the ratio between the sodium and potassium and the summation of them. Since it was confirmed that higher ratios of Na/K lower the temperature of vitrification and the shrinkage of the sintered body, while higher Na/K ratios may be causing the softening deformation due to the high sodium silicate of low melting point liquid phase formed [3–5].

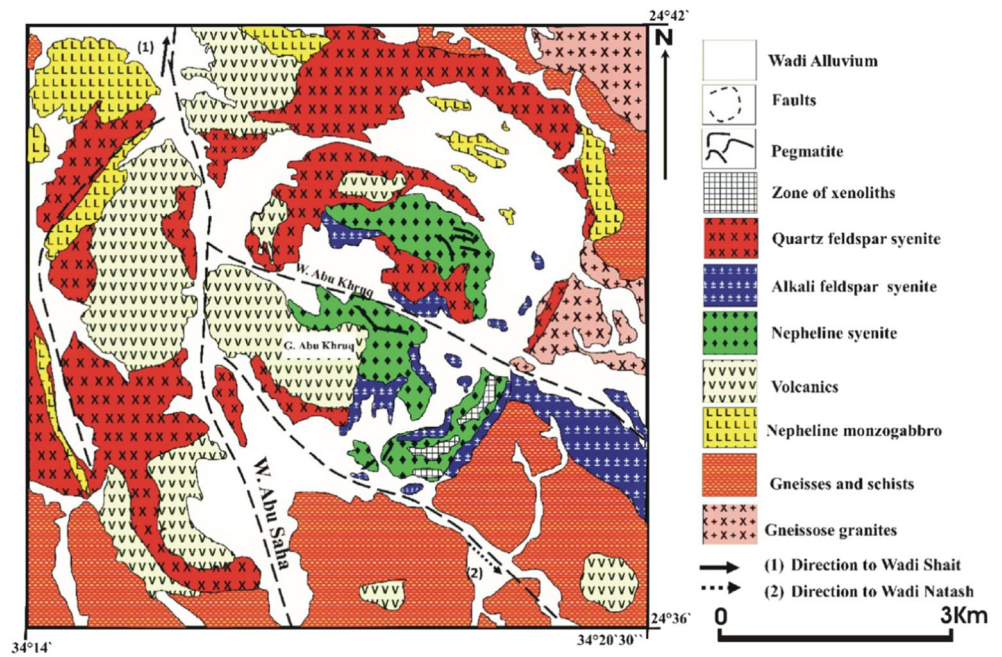
In order to avoid the expected shortage in the native pegmatite sodic and potassic feldspar, new sources should be prospected. The other sources of rocks containing feldspar and/or feldspathoids were investigated by several authors to assess their possibilities in utilizing as a flux in ceramic industry. One of the promising rocks containing both alkali feldspar are granitoids in addition to high quartz content, which is used as filler and supporting material for the

✉ A. I. M. Ismail  
aliism13@hotmail.com

<sup>1</sup> Refractories, Ceramics and Building Materials Department, National Research Centre, Dokki, Cairo, Egypt

<sup>2</sup> Geological Sciences Department, National Research Centre, Dokki, Cairo, Egypt

**Fig. 1** Geological map of the Abu Khruq area showing various lithologies (Mogahed, 2016)



ceramic tile body as well as forming a part of the liquid phase responsible for the densification of the ceramic body. Syenite rock types including syenite, quartz syenite and nepheline syenite, which contain high alkali content represented in nepheline and /or syenite for the sodic type as well as microcline for the potassium source. The high contents of alkalis and low content in quartz makes them the most promising rocks could be utilized in ceramic industries. Some researches were carried out for the utilization of nepheline syenite in ceramic tiles, it was found that 5.0% of

nepheline syenite are sufficient to accelerate the densification process. By increasing syenite content the vitreous phase in porcelain stoneware bodies increases, while the amounts of quartz and mullite are generally reduced. Further, the use of 10 wt.% of nepheline syenite were found to decrease the viscosity of glassy phase, which produces an enhanced shrinkage rate [6–8].

Extensive mining of nepheline syenite deposits has been found to occur mainly in Canada [7], Norway [9] and Russia [10], otherwise, it is limited and discontinuous in other

**Fig. 2** X-ray diffraction pattern of the nepheline syenite

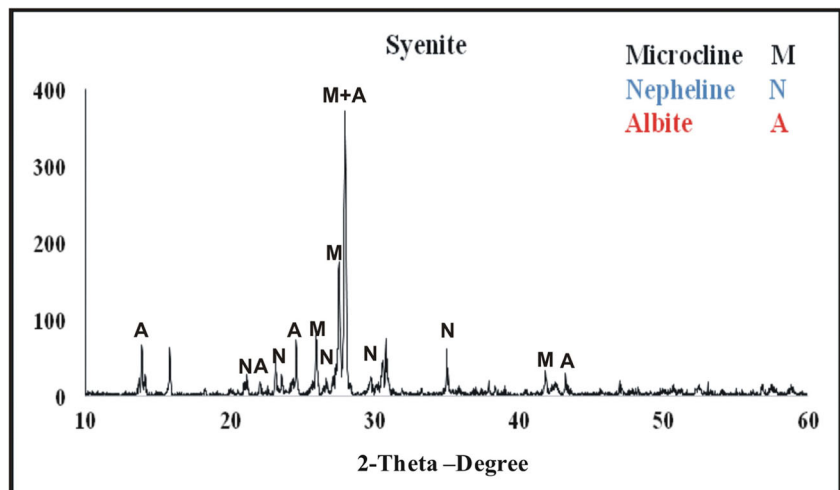
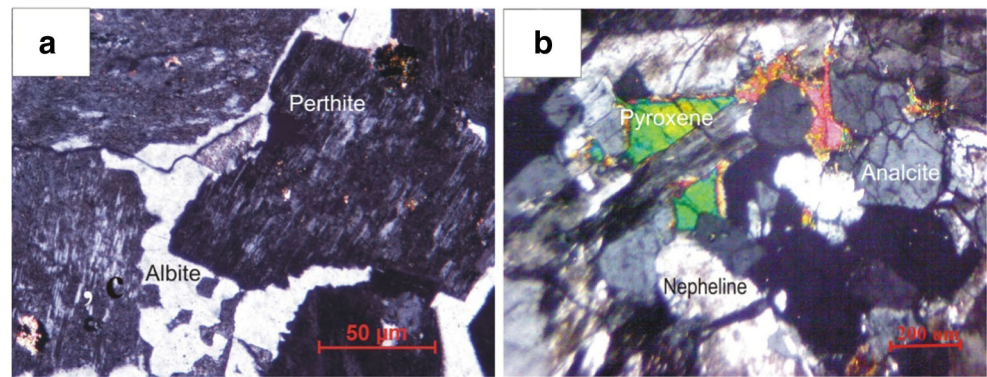


**Fig. 3** Microscopic photos of the Abu Khruq nepheline syenite



countries. However, the Russian nepheline syenite is mostly used locally for the alumina production. In Egypt, nepheline syenite is restricted to alkaline ring complexes that emplaced in the southern part of the Eastern Desert during the Phanerozoic anorogenic episode following the Pan-African orogeny [11]. In general, ring complexes are circular in shape and their principal rock units include syenogabbro, alkali syenites and nepheline syenites. They often contain alkali volcanic relics such as trachyte and trachybasalt. Abu Khruq ring complex, is one of the few promising occurrences in Egypt, is often preferred in the manufacture of ceramics replacing the currently used feldspar.

Gabal Abu Khruq ring complex exposes at longitude 34°18'08"N and latitude 24°38'55"E, north to the Aswan city between the Nile River and the Red Sea. It is formed of high relief hills reaching 900 m above sea level and covering an area of approximately 50 km<sup>2</sup>. The complex intrudes late Proterozoic Pan-African gneisses and schists and is dissected by a number of NW, NE and SW faults and crossed by dykes.

The Abu Khruq ring complex forms incomplete outer and inner ring structure of late Cretaceous age (~90 Ma); synchronous probably with major rifting of the south Atlantic belt [12]. It is occupied by alkali rocks, including gabbros, syenites and volcanics. The distribution of the *syenoid rocks* in relation to other lithological units is shown in Fig. 1. The *syenoids* show a compositional variation from quartz syenite to nepheline syenite. The under saturated

nepheline syenite is the latest formed phase and appears as a cone, elongated NW-trending body in the central part of the complex. It is light brown to gray and sheared where red ferruginated deuteritic alteration is commonly been attributed to the effect of Fe-rich hydrothermal solutions.

Several studies were done on the Abu Khruq nepheline syenite to reduce its colouring oxides as titanium and iron oxides to be adequate in porcelain tile production and they achieved a great success in terms of grinding and magnetic separation. However, Fe<sub>2</sub>O<sub>3</sub> content could decrease from 4.8% to 0.52% after using a single magnetic separation treatment [13], in agreement with the previous results [14–17].

The goal of the present work is to investigate the effect of adding different concentrations of syenite on the technological properties of the prepared ceramic tiles by testing some dry and firing parameters in addition to study the chemical and mineral composition of the raw materials as well as the phase composition and microstructure of the fired batches. To perform this purpose, four batches of the ceramic tiles were prepared, one blank without syenite and the other three ones with 5, 10 and 15% syenite replacing the feldspars to adjust the alkali percent in a nearly constant content.

## 2 Materials and Methods

The raw materials used in the present work comprise kaolin, quartz and feldspars in addition to nepheline syenite replacing the feldspars to establish the alkalis percent of the batches. The Kaolin, quartz and feldspar were provided by El-Nile Company for Mining, while syenite blocks are collected from Abu Khruq area, south Eastern Desert, Egypt. The petrographical, mineralogical and chemical characteristics of syenite as well as the phases formed during firing are carried out using transmitted light

**Table 1** Major oxides (wt.%) of the nepheline syenite

SiO <sub>2</sub>	TiO <sub>2</sub>	Al <sub>2</sub> O <sub>3</sub>	Fe <sub>2</sub> O <sub>3</sub>	MgO	CaO	Na <sub>2</sub> O	K <sub>2</sub> O	L.O.I	Total
56.90	0.05	22.64	2.78	0.30	0.56	9.34	4.95	1.25	98.77

**Table 2** Batch composition no. 1

Oxide%	Kaolinite 30%	Albite 25%	Potash feldspar 25%	Quartz 20%	total	Standard range
SiO <sub>2</sub>	13.58	18.35	16.10	18.60	66.63	65–67
TiO <sub>2</sub>	0.33	0.01	0.003	0.02	0.36	0.6–0.69
Al <sub>2</sub> O <sub>3</sub>	11.61	3.66	4.54	0.95	20.76	19.5–20.5
Fe <sub>2</sub> O <sub>3</sub>	0.13	0.02	0.06	0.008	0.22	0.69–0.77
MgO	0.02	0.03	–	0.002	0.05	0.66–0.69
CaO	0.04	0.16	0.06	0.004	0.26	0.60–0.77
Na <sub>2</sub> O	0.003	2.35	0.60	0.006	2.96	3.2–3.7
K <sub>2</sub> O	0.02	0.03	3.30	0.012	3.36	2.5–4.04
LOI	4.12	0.35	0.17	0.338	4.98	3.76–4.04
Total	29.93	24.96	24.83	19.94	99.58	99.97

microscope, XRD analysis within this study was conducted using a Philips X-Ray Diffraction equipment model X'Pert PRO with Monochromator, Cu-radiation ( $\lambda = 1.542 \text{ \AA}$ ) at 50 K.V., 40 M.A. and scanning speed  $0.02^\circ/\text{sec}$ . Were used. The reflection peaks between  $2\theta = 2^\circ$  and  $60^\circ$ , corresponding spacing ( $d$ ,  $\text{\AA}$ ) and relative intensities ( $I/I_0$ ) were obtained. The diffraction charts and relative intensities are obtained and compared with ICDD files. The XRF analysis was carried out for powder ( $< 74 \mu\text{m}$ ) samples using X-Ray fluorescence equipment PW 2404 with six analyzing crystals. Crystals (LIF-200), (LIF-220) were used for estimating Ca, Fe, K, Ti, Mn and other trace elements from Nickel to Uranium while crystal (TIAP) was used for determining Mg and Na. Crystal (Ge) was used for estimating P and crystal (PET) for determining Si and Al and PXI for determining Sodium and Magnesium. The Concentration of the analyzed elements is determined by using software SuperQ and SemiQ programs with accuracy 99.99% and

confidence limit 96.7%. The estimation of the major and trace elements were done as powder pellets (Pellets method) which were prepared by pressing the powder of the sample in Aluminum Cup using Herzog presser and 10 ton pressure. A scanning electron microscope (SEM) has been used in the present study for both textural analysis and mineralogical identification as well as microstructure. The very high resolution obtained in the SEM readily describes the minerals microstructure and microchemistry using the scanning electron microscope attached with EDX unit. The Scanning Electron Microscope using SEM Model Quanta 250 FEG (Field Emission Gun) attached with EDX Unit (Energy Dispersive X-ray Analyses), with accelerating voltage 30 K.V., magnification 14x up to 1,000,000. X-ray diffraction (XRD) and X-ray fluorescence spectrometer (XRF). The chemical analyses of Kaolin, quartz and feldspar raw materials had been determined before [18].

**Table 3** Batch composition no. 2

Oxide%	Kaolinite 30%	Albite 20%	Potash feldspar 25%	Quartz 20%	Syenite 5%	total	Standard range
SiO <sub>2</sub>	13.58	14.68	16.10	18.60	2.85	65.81	65–67
TiO <sub>2</sub>	0.33	0.01	0.003	0.02	0.003	0.37	0.6–0.69
Al <sub>2</sub> O <sub>3</sub>	11.61	2.93	4.54	0.95	1.13	21.16	19.5–20.5
Fe <sub>2</sub> O <sub>3</sub>	0.13	0.02	0.06	0.008	0.14	0.39	0.69–0.77
MgO	0.02	0.02	–	0.002	0.02	0.06	0.66–0.69
CaO	0.04	0.13	0.06	0.004	0.03	0.26	0.60–0.77
Na <sub>2</sub> O	0.003	1.88	0.60	0.006	0.53	3.02	3.2–3.7
K <sub>2</sub> O	0.02	0.02	3.30	0.012	0.25	3.60	2.5–4.04
LOI	4.12	0.28	0.17	0.338	0.07	4.98	3.76–4.04
Total	29.844	19.954	24.93	19.948	5.02	99.65	99.97



**Table 4** Batch composition no. 3

Oxide%	Kaolinite 30%	Albite 20%	potash feldspar 20%	Quartz 20%	Syenite 10%	total	Standard range
SiO <sub>2</sub>	13.58	14.68	12.882	18.60	5.69	65.43	65–67
TiO <sub>2</sub>	0.33	0.01	0.002	0.02	0.005	0.37	0.6–0.69
Al <sub>2</sub> O <sub>3</sub>	11.61	2.93	3.634	0.95	2.264	21.38	19.5–20.5
Fe <sub>2</sub> O <sub>3</sub>	0.13	0.02	0.048	0.008	0.278	0.48	0.69–0.77
MgO	0.02	0.02	–	0.002	0.03	0.07	0.66–0.69
CaO	0.04	0.13	0.048	0.004	0.056	0.28	0.60–0.77
Na <sub>2</sub> O	0.003	1.88	0.482	0.006	1.057	3.43	3.2–3.7
K <sub>2</sub> O	0.02	0.02	2.64	0.012	0.495	3.12	2.5–4.04
LOI	4.12	0.28	0.134	0.338	0.125	5.00	3.76–4.04
Total	29.844	19.954	19.94	19.948	10.00	99.56	99.97

The processing was done at the laboratory scale by milling the raw materials in wet condition (15 min in planetary mill with porcelain jar and porcelain grinding media). The slip so obtained (~70% solid load, 0.3% Na-tripolyphosphate) was oven dried and disagglomerated (agate mortar) prior manual granulation (sieve 2 mm, powder moisture ~5 wt%). Powders were shaped into 30 × 30 × 5 mm tiles by hydraulic pressing (35 MPa), then dried in an oven (110 °C overnight) and fast fired in electric furnace (max. Temperature from 1160 °C to 1260 °C; 30 min soaking time). Some technological behaviors of the samples were determined in dry state and after firing at 1260 °C; 30 min. The linear shrinkage and bulk density were measured for the dry samples, while the technological properties were determined for the fired tiles including linear shrinkage, water absorption, apparent porosity and bulk density. Sintering curves were drawn using linear shrinkage, water absorption, porosity and bulk density versus the firing

temperatures. Phase composition and microstructure analysis of the batches fired at 1260 °C were detected using XRD and SEM with EDX, respectively. Whiteness of the fired batched is measured by DRK 103A Whiteness meter, this meter is designed according to GB3978–83 standard lighting substance and lighting observation condition, modeling D65 lighting. It adopts d/o lighting observing geometry terms (ISO 2469).

### 3 Results

#### 3.1 Characterization of the raw Materials

The mineral and chemical compositions of kaolin, quartz and feldspar samples have been studied [18]. The authors found that the kaolin is composed mainly of kaolinite with minor amount of quartz, while quartz is made of a majority of quartz

**Table 5** Batch composition no. 4

Oxide%	Kaolinite 30%	Albite 15%	Alkali feldspar 20%	Quartz 20%	Syenite 15%	total	Standard range
SiO <sub>2</sub>	13.58	11.01	12.882	18.60	8.535	64.61	65–67
TiO <sub>2</sub>	0.33	0.01	0.002	0.02	0.0075	0.37	0.6–0.69
Al <sub>2</sub> O <sub>3</sub>	11.61	2.20	3.634	0.95	3.396	21.79	19.5–20.5
Fe <sub>2</sub> O <sub>3</sub>	0.13	0.01	0.048	0.008	0.417	0.61	0.69–0.77
MgO	0.02	0.02	–	0.002	0.045	0.09	0.66–0.69
CaO	0.04	0.10	0.048	0.004	0.084	0.28	0.60–0.77
Na <sub>2</sub> O	0.003	1.41	0.482	0.006	1.5855	3.49	3.2–3.7
K <sub>2</sub> O	0.02	0.02	2.64	0.012	0.7425	3.44	2.5–4.04
LOI	4.12	0.21	0.134	0.338	0.1875	4.99	3.76–4.04
Total	29.844	14.99	19.94	19.948	15.00	99.56	99.97

**Table 6** Bulk density and shrinkage of the green batches

batch	1	2	3	4
Bulk density g/cm <sup>3</sup>	1.87	1.90	1.88	1.87
Shrinkage %	+2.60	+2.53	+2.63	+2.67

with minor kaolinite. Sodic feldspar is formed of albite and quartz, while the potash rich type is mainly orthoclase with few albite. The chemical compositions of the raw materials used in the present study confirm their mineralogical compositions for the silica and alumina of the kaolin and quartz, and the alkali contents for the alkali feldspars.

Nepheline syenite as estimated by XRD is dominated by alkali feldspars (albite as the main sodic feldspar and microcline as potash feldspar) as well as feldspasoids (nepheline as the essential sodic feldspathoids) (Fig. 2). Petrography, as confirmed by microscopic study, nepheline syenite is medium-grained rock having an equigranular texture and consisting of alkali feldspars (mainly microcline-perthite-albite) (65–80 model %), nepheline (7–15 model %), aegirine -augite (8–12 model %) and analcite (0–3 model %). The main accessories are amphibole, apatite, zircon and opaques. The crystals of these rocks are dominantly subhedral to anhedral with grain size of 2–5 mm. The alkali feldspar is mainly represented by microcline which shows cross-hatch twinning or intergrows with the albite in the form of patchy perthitic intergrowths (Fig. 3a). Sometimes microcline contains mafic minerals and opaque inclusions and altered to sericite. Alkali sodic pyroxene (aegirine-augite, aegirine) is the dominant mafic mineral in the chose samples (Fig. 3b), rarely overgrown by amphibole. Nepheline commonly corrodes and replaces feldspars or fills in association with analcite the interstices between the early formed minerals. It is altered to minute micaceous and zeolitic materials.

**Table 7** Bulk density of fired batches up to 1260 °C

Firing temperature	1	2	3	4
1160	1.82	1.94	2.02	2.08
1180	2.02	2.05	2.09	2.19
1200	2.04	2.09	2.11	2.19
1220	2.06	2.10	2.06	2.16
1240	2.08	2.10	2.10	2.12
1260	2.11	2.10	2.00	2.02

**Table 8** Apparent porosity of fired batches up to 1260 °C

Firing temperature	1	2	3	4
1160	26.0	23.34	21.96	21.25
1180	17.16	15.03	12.14	10.19
1200	9.49	8.82	8.28	8.24
1220	7.08	7.77	7.00	8.00
1240	4.06	7.03	6.51	4.35
1260	3.58	5.93	4.47	5.00

Chemically, the analyzed nepheline syenite contains silica content 56.90%, and has high Al<sub>2</sub>O<sub>3</sub> (22.64%) and high total alkalis (Na<sub>2</sub>O 9.34%, K<sub>2</sub>O 4.95%) contents, and reasonable Fe<sub>2</sub>O<sub>3</sub> (2.78%) and TiO<sub>2</sub> (0.05%) contents. Total MgO + CaO is less than 1% and loss on ignition is 1.25% (Table 1).

### 3.2 Batch Materials

Four batches of the ceramic tiles were designed to achieve the main chemical composition of the porcelain and ceramic bodies and to adjust the chemical composition in a proper chemical content.

Table 2 illustrates the chemical and phase compositions of the batch no. 1 that was designed to have kaolin 30%, sodic and potash feldspar 25% for each of them, in addition to quartz 20%. The range of chemical composition to achieve the standard composition of the ceramic tile batch is silica 66.63%, Al<sub>2</sub>O<sub>3</sub> 20.76%, Na<sub>2</sub>O 2.96% and K<sub>2</sub>O 3.36%, with total impurity oxides less than 1% and loss on ignition 4.98%.

Table 3 shows the batch composition and the chemical composition of batch no. 2. By adding 5% syenite, the albite content decreases to 20% while the potash feldspar, kaolin and quartz keep with their percentage contents as 25, 30 and

**Table 9** Water adsorption of fired batches up to 1260 °C

Firing temperature	1	2	3	4
1160	13.83	12.03	10.87	10.22
1180	8.50	7.33	5.81	4.45
1200	4.41	3.81	3.82	3.68
1220	4.17	3.79	3.37	3.12
1240	1.97	3.29	3.16	2.01
1260	1.75	2.78	2.24	2.70

**Table 10** Linear shrinkage of fired batches up to 1260 °C

Firing temperature °C	1	2	3	4
1160	+0.87	+0.43	−0.13	+0.13
1180	1.70	2.0	2.53	2.87
1200	2.24	2.83	4.13	4.67
1220	3.07	2.86	3.6	4.13
1240	3.60	2.97	3.17	3.96
1260	4.07	3.13	2.67	1.77

30%, respectively. This batch composition establishes the chemical composition within the range as silica 65.81%,  $\text{Al}_2\text{O}_3$  21.16%,  $\text{Na}_2\text{O}$  3.02% and  $\text{K}_2\text{O}$  3.60%, in addition to the total impurity oxides less than 1% and loss on ignition 4.98%.

In batch no. 3, the syenite content increases to 10% at the expense of sodic and potash feldspars which become 20% for both feldspars. In the other hand, kaolin and quartz are represented by the same percents as 30% and 20%, respectively. This calculated composition confirms the chemical composition as silica 65.43%,  $\text{Al}_2\text{O}_3$  21.38%,  $\text{Na}_2\text{O}$  3.43% and  $\text{K}_2\text{O}$  3.12%, besides the total impurity oxides is less than 1% and loss on ignition 5.00% (Table 4).

Batch no. 4 shows the batch composition of 15% nepheline syenite together with 15% albite and 20% potash feldspar. The kaolin and quartz have the same percentages as before 30 and 20%, respectively. The chemical composition of this batch displays silica 64.61%,  $\text{Al}_2\text{O}_3$  21.79%,  $\text{Na}_2\text{O}$

3.49% and  $\text{K}_2\text{O}$  3.44%, with total impurity oxides slightly more than 1% and loss on ignition 4.99% (Table 5).

### 3.3 Densification Parameters

The four batches were fired up to 1260 °C and the densification parameters were recorded. Table 6 shows bulk density and shrinkage of the green batches after overnight drying at 110 °C. The bulk densities of the four batches range from 1.87 to 1.90  $\text{g}/\text{cm}^3$ , while shrinkage was within +2.53 and +2.67 as expansion.

Densification parameters (e.g. bulk density, apparent porosity, water absorption ...etc) of the fired batches at 1260 °C are measured and shown in Tables 7, 8, 9 and 10 and Figs. 4, 5 and 6).

Bulk density of the batch no. 1 increases gradually from 1160 °C to 1260 °C as 1.82  $\text{g}/\text{cm}^3$  and 2.11  $\text{g}/\text{cm}^3$ , respectively, while batch no. 2, which contains 5% of syenite, raises from 1160 °C to 1220 °C as 1.94  $\text{g}/\text{cm}^3$  and 2.1  $\text{g}/\text{cm}^3$ , and still constant up to 1260 °C. By increasing the syenite percent to 10 and 15%, the bulk density increases to 2.11 and 2.19  $\text{g}/\text{cm}^3$  at 1200 °C, respectively (Table 7 and Fig. 3).

Apparent porosity decreases with increasing firing temperature from 1160 °C to 1260 °C to the minimum values as 3.58, 5.93 and 4.47% for batch nos. 1, 2 and 3, respectively. But for the batch no. 4 containing 15% syenite, the minimum porosity obtained at 1240 °C is 4.35% and increases to 5.00% at 1260 °C (Table 8 and Fig. 4).

Water adsorption shows gradual decrease from 1160 °C to 1260 °C for the batch nos. 1, 2 and 3 as 1.75, 2.78 and 2.24%,

**Fig. 4** Bulk density of the ceramic tile batches at temperatures of 1160 °C to 1260 °C

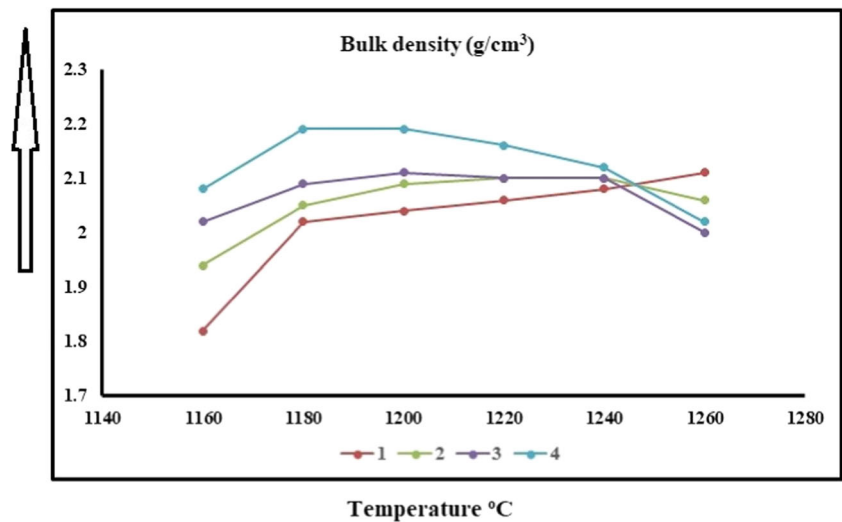
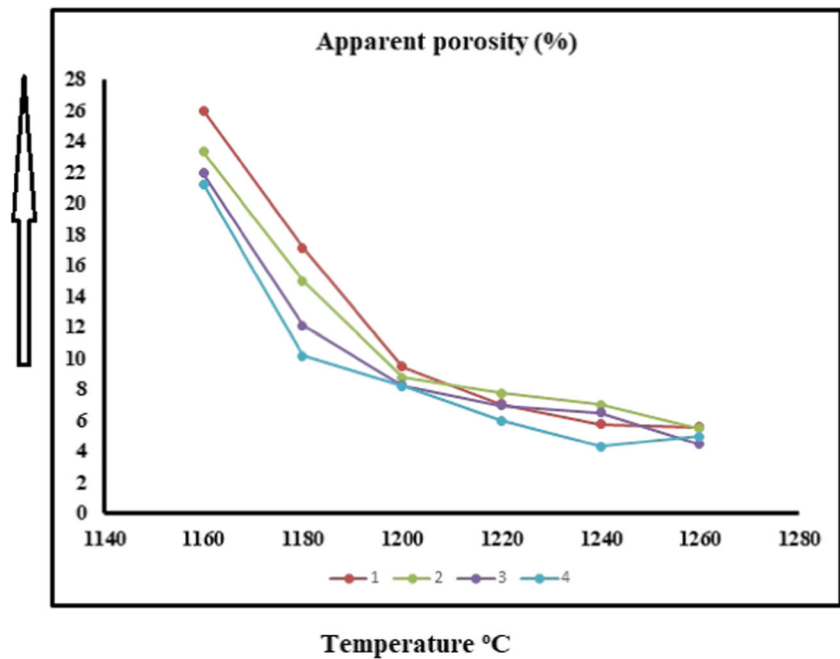


**Fig. 5** Apparent porosity of the ceramic tile batches at temperatures of 1160 °C to 1260 °C



while the batch no. 4 has the minimum water adsorption at 1240% as 2.01% and slightly increases to 2.70% at 1260 °C, (Table 9 and Fig. 6).

The whiteness of the four batches is investigated to detect the effect of the syenite content on the whiteness degree. It is obvious that by increasing the syenite from 0% to 15%, the whiteness degree decreases in the order 52.39, 45.56, 41.40 and 36.65 for the batches 1, 2, 3 and 4, respectively (Table 10). This can be described to the colouring oxides of the syenite.

### 3.4 Shrinkage Characteristics

Linear shrinkage defines as the decrease in length of a fine-grained soil mass when oven-dried and its moisture content is reduced from liquid limit to an oven-dry state. Shrinkage is determined at temperatures more than 1000 °C, at which the glassy phase is formed and mullite phase re-crystallizes.

Table 11 and Fig. 7 show the relation between linear shrinkage of the various batches and firing temperatures up

**Fig. 6** Water adsorption of the ceramic tile batches at temperatures of 1160 °C to 1260 °C

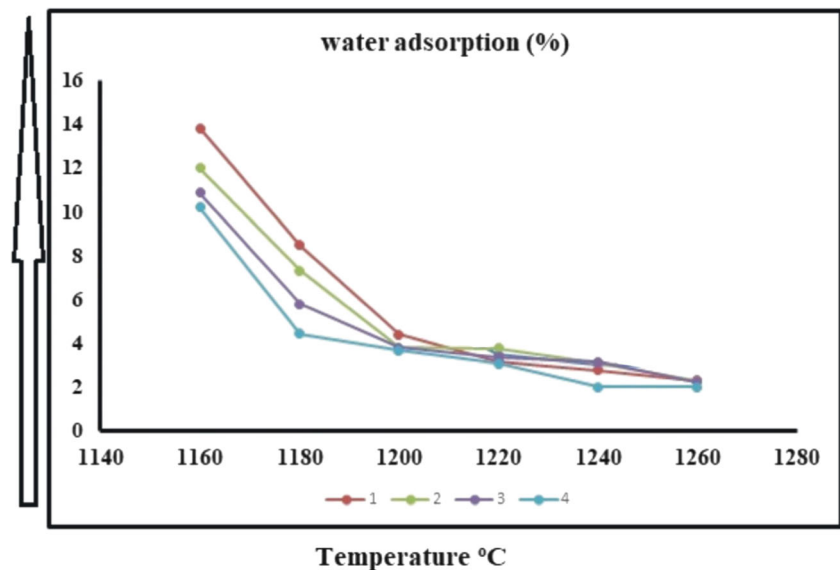




**Table 11** Whiteness of fired batches at 1260 °C

Firing temperature °C	1	2	3	4
1260	52.39	45.56	41.40	36.65

to 1260 °C. It is clear that shrinkage displayed by batches 1 and 2 increases gradually from +1.77 to 4.24% at 1160 °C to 1260 °C, respectively. On the other hand, batches 3 and 4 show the maximum shrinkage at 1240 °C as 3.17% and 3.96%, respectively, then shrinkage begins to decrease at 1260 °C to 2.67% and 1.77%.

### 3.5 Microstructures

Figures 8 and 9 exhibit the microstructures of the fired batches 1 and 4 at 1260 °C as recognized by scanning electron microscope. Both batches show microstructure consisting of primary mullite set in a matrix of siliceous glassy phase. Furthermore, primary mullite crystals are recorded in two forms; crystalline coarse grains and small rounded grains [19].

Phase composition of the batches 1 and 4 at firing temperature 1260 °C was estimated using XRD technique. The X-ray patterns refer to the occurrence of both mullite and quartz as the essential phases in the two batches in addition to few albite phase in batch no. 1 (Fig. 10).

The composition of the four batches was designed to have the standard range of the ceramic tiles since silica 65–67%,

alumina 19.5–20.5%, fluxing oxides Na<sub>2</sub>O 3.2–3.7% and K<sub>2</sub>O 2.5–4.04%, and other oxides do not exceed 1.0%.

## 4 Discussion

The batches were fired in the temperature range of 1160 °C to 1260 °C and the densification parameters of the batches were measured. It was noticed that by increasing the firing temperature, the bulk density and linear shrinkage of pellets increase, while the porosity and water adsorption decrease being due to the beginning of liquid phase formation of the sodic feldspar at ~985 °C in addition to the meta-kaolin reactions. Sodic feldspar completely melts at 1118 °C and potash feldspar at 1150–1175 °C, which filled the pores and densified the bodies. The decrease in density at 1240 °C results from gas release that leads to the formation of bubbles in the microstructure and increase in porosity. Furthermore, secondary mullite crystals grow from the outer surface of the clay relict into the feldspar relict suggesting that primary mullite may act as a seed for the nucleation of secondary mullite [20].

Mullite is the main development phase formed after firing and recorded with the glassy phase in both phase compositions carried out by XRD as well as the SEM and EDAX, whereas quartz is the main constituents in the batch compositions. The transformation of kaolin to meta-kaolin and by firing temperature to mullite and silica, which react with the feldspar to form the high content of liquid phase. However, diffusion process depends on

**Fig. 7** linear shrinkage of the ceramic tile batches at temperatures of 1160 °C to 1260 °C

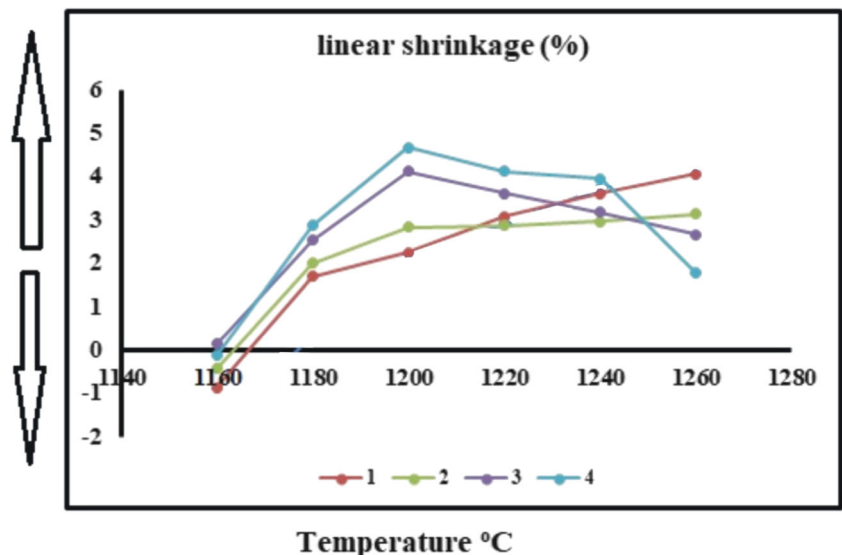
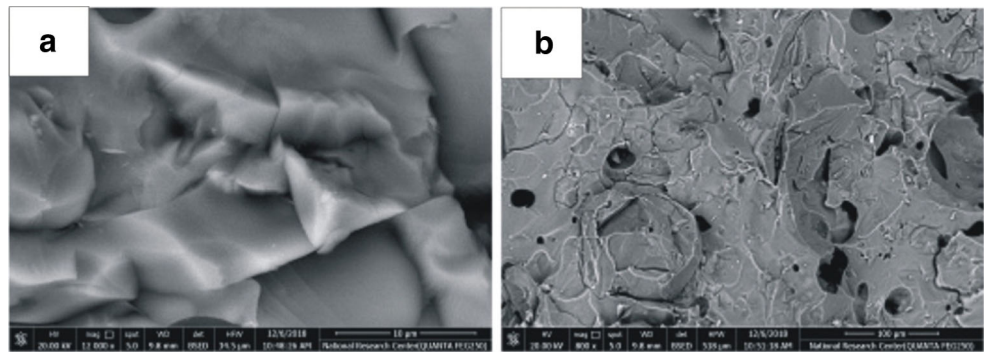


**Fig. 8** SEM images of the designed batch 1 fired at 1260 °C: a Interlocking primary mullite crystals; b Primary mullite embedded in a glassy matrix

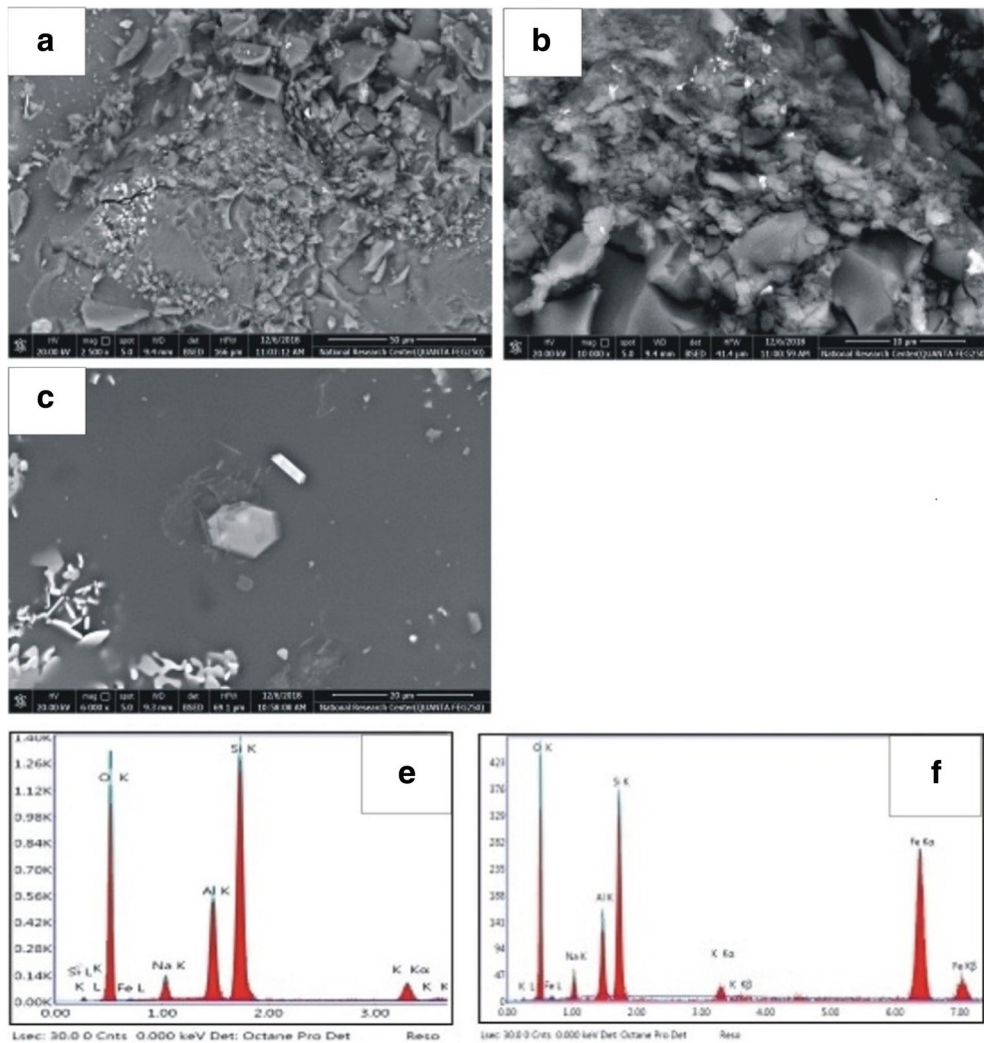


the concentration gradients and the diffusion rates of  $K_2O$  and  $Al_2O_3$ .

These results show that nepheline syenite has a significant effect on the sintering rate and influences

remarkably on the sintering behavior; increasing the shrinkage and decreasing total porosity. On the other hand, with increasing the nepheline syenite, the alkali contents increase and the liquid phase increases at the

**Fig. 9** Microstructure and EDEX of the designed batch 4 fired at 1260 °C. a & b Clusters mullite embedded in a glassy matrix; c coarse grained mullite crystals with interstitial pores; d few tabular crystals of feldspar rich in iron; e & f EDEX and semi-quantitative analyses of the fired batch 4



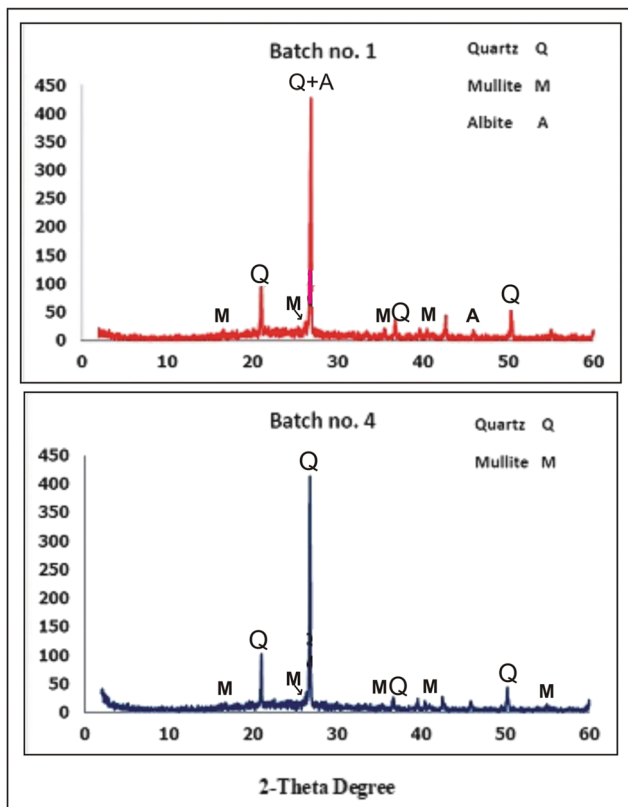


Fig. 10 X-ray spectra of the batches 1 and 4 fired at 1260 °C

expense of mullite and quartz. The bodies rich in nepheline syenite show large amounts of glassy phase. These bodies also present lower whiteness with the same sintering conditions. The colorant characteristics appear to be directly related to the colouring oxides, which are represented by the iron and titanium oxides [21].

## 5 Conclusion

Chemical and mineral composition of the raw materials including kaolin, sand, albite, potash feldspar was previously performed in previous work, while syenite was investigated in this work.

Mineralogically, syenite is essentially composed of microcline, albite and nepheline together with few pyroxene and analcite.

Four batches with different concentrations of nepheline syenite (0, 5, 10 and 15%) were prepared.

The four batches were fired from 1160 to 1260 °C with interval 20 °C.

Phase composition carried out by XRD and microstructural analyses by SEM and EDAX demonstrated that mullite is the main newly formed phase after firing embedded in an alkali-rich glassy mass while quartz is the main mineral in batch composition.

Technological properties of the fired batches proved that increasing the firing temperature and nepheline syenite contents caused increasing in the amounts of the produced glassy phase, and consequently the bulk density and linear shrinkage increased but apparent porosity and water adsorption as well as whiteness of fired batches decreased.

It is finally obvious that nepheline syenite could be successfully used as flux in ceramic tiles but it is not accepted in the manufacturing of porcelain bodies being due to their coloration.

## References

1. Carty WM, Senapati U (1998) Porcelain-raw materials, processing, phase evolution and mechanical behavior. *J Am Ceram Soc* 81:3–20
2. Iqbal Y, Lee EJ (2000) Microstructural evolution in triaxial porcelain. *J Am Ceram Soc* 83:3121–3127
3. Harben PW (1995) World distribution of industrial mineral deposits. *The industrial minerals handbook*, London industrial mineral division, Metal Bulletin PLC, pp. 15–31
4. Dondi M (2018) Feldspathic fluxes for ceramics. Sources, production trends and technological value. *Resour Conserv Recycl* 133: 191–205
5. El-Fadaly E (2018) Characterization of porcelain stoneware tiles based on solid ceramic wastes. *Environ Sts Res Inst, El-Sadat City Univ, El-Menofia, Egypt, Period Mineral* 87:67–81
6. Esposito L, Salem A, Tucci A, Gualtieri A, Jazayeri SH (2005) The use of nepheline-syenite in a body mix for porcelain stoneware tiles. *Ceram Int* 31:233–240
7. Payne JG (1968) Geology and geochemistry of the Blue Mountain nepheline syenite. *Can J Earth Sci* 5:259–273
8. Serencsits C, Faul H, Foland K, Hussein A, Lutz T (1981) Alkaline ring complexes in Egypt: their ages and relationship in time. *J Geophys Res Solid Earth* 86:3009–3013
9. Geis HP (1979) Nepheline syenite on Stjerneoy, northern Norway. *Econ Geol* 74:1286–1295
10. Nedosekova IL, Vladykin NV, Pribavkin SV, Bayanova TB (2009) The Il'mensky-Vishnevogorskymiaskite-carbonatite complex, the Urals, Russia: origin, ore resource potential, and sources. *Geol Ore Depos* 5:139–161
11. Bowden P (1985) The geochemistry and mineralization of alkaline ring complexes in Africa (a review). *J Afr Earth Sci* 3:17–39
12. Vail JR (1989) Ring complexes and related rocks in Africa. *J Afr Earth Sci* 8:19–40
13. Ismail AIM, Sadek Ghabrial D, Abdel Wahab W, Eissa M, Cazzaniga A, Zanelli C, Dondi M (2018) Exploring Syenites from ring complexes in the Eastern Desert (Egypt) as ceramic raw materials. *Period Mineral* 87:67–81

14. Abouzeid AM, Negm AA (2014) Characterization and beneficiation of an Egyptian nepheline Syenite Ore. Hindawi publishing corporation, *inter J mineral*, Article ID 128246, 2014: 1–9
15. Mogahed MM (2016) Petrogenesis of cogenetic silica-oversaturated and -undersaturated syenites of Abu Khruq ring complex, south Eastern Desert, Egypt. *J Afr Earth Sci* 124:44–62
16. Partyka J, Sabet B, Gajek M (2012) Technological study and characterization of weathered syenite. *Interceram* 61:101–105
17. Zanelli Z, Soldati R, Conte S, Guarini G, Ismail AIM, El-Maghraby MS, Cazzaniga A, Dondi M (2019) Technological behavior of porcelain stoneware bodies with Egyptian syenites. *Int J Appl Ceram Technol* 16(2):574–584
18. El-Maghraby MS, Ismail AIM, Shalaby B Utilization of some Egyptian raw materials in ceramic tiles. *Bull Nat Res Centre* (In Press)
19. Kunduraci N, Aydin T, Akbay A (2016) The effect of nepheline Syenite addition on the sintering behaviour of Sanitaryware bodies. *J Australian Ceram Soc* 52:82–86
20. Salem A, Jazayeri SH, Rastelli E, Timellini G (2009) Dilatometric study of shrinkage during sintering process for porcelain stoneware body in presence of nepheline. *J Mater Process Technol* 209:1240–1246
21. Salem A, Jazayeri SH, Rastelli E, Timellini G (2009) Effect of nepheline syenite on the colorant behavior of porcelain stoneware body. *J Ceram Process Res* 10:621–627

**Publisher's Note** Springer Nature remains neutral with regard to jurisdictional claims in published maps and institutional affiliations.